The HEARTS EU Project and its Initial Results on Fragmented High-Energy Heavy Ion Single Event Effects Testing

Rubén García Alía *Member, IEEE*, Andreas Waets, Andrea Coronetti, Kacper Bilko, Marc Delrieux, Natalia Emriskova, Luigi Esposito *Member, IEEE*, Matthew Fraser, Eliott Johnson, Karolina Klimek, David Lucsanyi, Daniel Prelipcean, Mario Sacristán Barbero, Daniel Söderström *Member, IEEE*, Salvatore Danzeca, Federico Ravotti *Member, IEEE*, Simone Gilardoni, Francesco Cerutti, Marco Durante, Christoph Schuy, Tim Wagner, Ulrich Weber, Marta Bagatin *Member, IEEE*, Simone Gerardin *Member, IEEE*, Stefano Francola, Roberta Mancini, Renaud Mangeret *Member, IEEE* and Mirko Rostewitz

***Abstract*—We perform Single Event Effects (SEE) tests with well-characterized fully fragmented (i.e., beyond Bragg peak) high-energy heavy-ion beams and compare the results with those expected from conventional, mono-Linear Energy Transfer (LET) measurements, showing a satisfactory level of agreement between the two. This compliance paves the way to the exploitation of simulation tools for accurately quantifying the ion fragmentation impact on SEE rates for both ground-level testing conditions and space Galactic Cosmic Ray environments with electronics operating behind significant thicknesses of shielding. The satisfactory agreement level is also encouraging in view of the possible usage of fragmented heavy ion beams for ground-level SEE testing of electronics.**

***Index Terms*—CERN, electronics testing, high-energy heavy ions, single event effect (SEE), single event upset (SEU), nuclear reactions, Monte Carlo simulations.**

I. Introduction

The European Union (EU) funded "High-Energy Accelerators for Radiation Testing and Shielding" (HEARTS) project [1] is aimed at enhancing Europe's capacity of replicating Galactic Cosmic Ray (GCR) conditions and effects at ground level for shielding, radiobiology and microelectronics testing applications. The 4-year project, which was kicked-off in January 2023, incorporates CERN and GSI as accelerator infrastructures (along with their radiation effects knowledge and experience), and the University of Padova (UNIPD), Thales Alenia Space (TAS) and Airbus Defence and Space (including the participation of TESAT) as academic (the first) and industrial (the last two) radiation effects experts and experienced radiation testing users.

In particular and as to what concerns electronics testing, HEARTS directly addresses the need of higher energy heavy-ion beams to cope with the qualification of advanced components with complex packaging and/or assembly structures [2], [3], enabling their use for space applications. This need is becoming increasingly important with the advancement of commercial microelectronic technologies as well as their stronger relative presence in space missions. In other words, some of the microelectronics devices and assemblies that could act as enablers for a variety of advanced space applications (e.g., on-board artificial intelligence) cannot be tested in standard energy (up to 10-20 MeV/n) cyclotron heavy-ion facilities due to the limited penetration of the ions.

Within CERN and as part of HEARTS' Work Package (WP) 7, the main objective is to offer well-characterized high-energy heavy-ion beams to electronics users. Such high-energy SEE testing capability development and validation are currently underway, and are expected to be finalized by the end of the project in December 2026, after which the electronics user access is expected to be maintained in a self-sustainable manner both for industrial and academic users. The WP7 activity focuses on high-energy (> 100 MeV/n) heavy-ion (mainly lead) beams produced at the CERN Proton Synchrotron (PS) accelerator and slow extracted (i.e., extracted over multiple accelerator turns [4], which is necessary for electronics testing in order to avoid the accumulation of the full beam pulse in a tens of ns time frame) in a spill of $\sim$ 300 ms to the East Area experimental hall [5], [6], through the F61 and T8 beam lines. Within CERN, this activity is the continuation of the ESA-funded CHIMERA efforts during 2021 and 2022, summarized in [7]. And, in turn, the CHIMERA activity was a follow-up of the 2017 and 2018 (i.e., two final CERN Run 2 years, before the Long Shutdown 2 in 2019 and 2020) proof-of-concept of high-energy heavy ion extraction and transport from the PS to the CHARM irradiation station [8], [9], albeit without energy

Manuscript submitted July 19, 2024.

R. García Alía (ruben.garcia.alia@cern.ch), A. Waets, A. Coronetti, K. Bilko, M. Delrieux, N. Emriskova, L. Esposito, M. Fraser, E. Johnson, K. Klimek, D. Lucsanyi, D. Prelipcean, M. Sacristán Barbero, D. Söderström, S. Danzeca, F. Ravotti, S. Gilardoni and F. Cerutti are with CERN, CH-1211, Genève, Switzerland.

K. Bilko is with the Univ Lyon, UJM-Saint-Etienne, Laboratoire Hubert Curien UMR 5516, F-42023, Saint-Étienne, France.

A. Coronetti and M. Sacristán Barbero are with the Institute d'Électronique et des Systèmes, Université de Montpellier, 34090 Montpellier, France.

D. Prelipcean is with the Physics Department, Technical University of Munich (TUM), Arcisstraße 21, 80333 München, Germany. Daniel's work is sponsored by the Wolfgang Gentner Programme of the German Federal Ministry of Education and Research (grant no. 13E18CHA).

A. Waets is with the University of Zurich, 8006 Zurich, Switzerland.

M. Durante, C. Schuy, T. Wagner and U. Weber are with GSI Helmholtzzentrum für Schwerionenforschung, 64291 Darmstadt, Germany.

M. Bagatin and S. Gerardin are with DEI - Padova University, via Gradenigo 6B Padova, PD 35131, Italy.

S. Francola and R. Mancini are with Thales Alenia Space Italy (TASI), Via Saccomuro, 24, 00131 Rome, Italy.

R. Mangeret is with Airbus Defence and Space, 31, Avenue des Cosmonautes 31402, Toulouse, France. Toulouse.

M. Rostewitz is with Tesat-Spacecom, Gerberstraße 49, 71522 Backnang, Germany

This work has been funded by the European Union under Grant Agreement No. 101082402 (the HEARTS project), through the Space Work Programme of the European Commission.

and flux control, both incorporated during the Run 3 (as of 2021 onwards) phase of the activity.

The HEARTS electronics testing activities at CERN were concentrated during the 2-week HEARTS@CERN campaign in October 2023. This campaign was mainly devoted to beam development and characterization efforts, the latter involving also instrumentation and experts from outside CERN, namely from GSI, the University of Oldenburg, PTW and the University of Wollongong. The beam characterization instruments and dosimeters used in addition to those permanently installed in the experimental beam line included a solid-state silicon detector [10], a silicon-on-insulator microdosimeter [11], a pixelized ionization chamber [12], several small ionization chambers (pinpoint, farmer) calibrated against high-energy heavy ions and (finally) SRAMs through which the LET of the beam can be extracted from the obtained Multiple Cell Upset (MCU) distribution [13].

In addition to the beam characterization activities completed during the 2023 HEARTS@CERN run, Single Event Effect (SEE) validation measurements were also performed by the CERN team, as presented in [14]. For these measurements, the average lead beam energy was set through a combination of accelerator and degrader configurations, and varied in an energy range from 1690 MeV/n (corresponding to a Linear Energy Transfer [LET] of 10.3 MeVcm^2/mg) down to 85 MeV/n (corresponding to an LET of 39.9 MeVcm^2/mg), in both cases at Device Under Test (DUT) surface level.

Along with the attractive opportunities high-energy heavy ion testing offers, it also poses some specific challenges associated to it, which are not directly covered in the existing SEE standards and guidelines. For instance, as detailed in [15], most heavy ion SEE tests are performed at facilities with beam ranges from 10s to 100s of microns, requiring device delidding prior to irradiation. Consequently, existing good practices, guidelines and standards for SEE testing are strongly focused on such type of heavy ion beams and facilities.

One of these challenges, as covered in Section II, is related to the fragmentation processes these ions will undergo and their possible impact on the SEE experiments. Another challenge, as further detailed in Section III, is linked to the physical trade-off between the accuracy of the LET value on its sensitive volume and its absolute magnitude. These challenges serve as motivation to the study presented in this work, which consists in utilizing a fully fragmented high-energy heavy ion beam, described in Section IV, to assess its impact on SEE induction, through the experimental results presented in Section V, and compared with those derived from the radiation-matter interaction simulation of the fragmented beam.

The results of the study and its Radiation Hardness Assurance (RHA) implications are then discussed in Section VI, with Section VII summarizing the conclusions and outlook of the work.

II. High-energy heavy ion fragmentation SEE impact

In practical terms and as introduced above, one of the key challenges related to the utilization and manipulation (e.g., through degraders and masks) of high-energy heavy ions is related to the fragmentation process they will undergo, which results in the generation of highly energetic and forwardly directed fragments that become a constituent (and therefore, in many cases, a contaminant) of the beam. In other words, experimental high-energy heavy ion beams will typically travel through long distances and non-negligible amounts of materials, in the form of vacuum windows, beam instruments, degraders, electronic boards, component packages and other overlayers (e.g., heat sinks), etc. This will result in the generation of secondaries through fragmentation, which will have a wide LET distribution, and which can induce SEEs both in the DUT as well as in the surrounding electronics (i.e., the part of the experimental setup which is not meant to be irradiated). Therefore, quantifying the SEE impact of these fragments and making sure that (a) their effect on the DUT is negligible in comparison to the primary beam and that (b) the impact on the surrounding electronics does not have a negative effect on the experiment execution, is essential for an efficient and accurate exploitation of such beams.

Moreover, the adequate characterization of the high-energy heavy ion fragmentation process and its impact on the SEE rate is also relevant in the context of space environment and effects, for cases in which ions would traverse significant amounts of material (e.g., in Lunar or Martian habitat shielding structures) before reaching the electronic devices and systems. Furthermore and as shown in [16], fragmented beams could also be of practical interest for radiation effects testing.

With the motivations above in mind, this work is devoted to the experimental and simulated assessment of the impact of fully fragmented beams on Single Event Upset (SEU) rates in three different commercial SRAM devices.

The importance of adequately simulating SEE rates from high-energy heavy ion fragments was extensively motivated in [17], in which discrepancies between different nuclear physics models in energy deposition distributions and hence SEE rates were highlighted. However, that work focused on energy deposition distributions in micrometric volumes without any surrounding material, and which are therefore dominated by low-energy, target-like recoils. Likewise, previous work on the subject of experimental and simulated heavy ion nuclear reaction induced Single Event Effects [18]–[24] also largely focused on micrometric structures and energies below 100 MeV/n, for which the deposited energy from nuclear reaction products is dominated by high-LET, low range secondaries.

In contrast to previous publications, the study included in this work focuses on geometries in the meter scale, in which the effect of high-energy nuclear reactions is dominated by projectile-like, high-energy fragments.

The SEE impact of such fragments was studied through a combination of experimental and simulation works in [25] and [26], using ultra-high energy heavy ion beams in the SPS North Area at CERN [27], [28]. In such cases, it was shown that the impact of high-energy heavy ion fragments on the total SEE rates was far from negligible, posing significant limitations to the usage of such beams for quantitative radiation effects testing. In other words, the applicability of an SEE

measurement in which the contribution to the events comes from a combination of the primary beam and its fragments is quite limited, as it cannot be used for predicting SEE rates in a different environment.

In this work, the main approach and novelty is to perform SEE measurements with fully fragmented beams, i.e., beams for which the primary particles have either undergone fragmentation, or have been ranged out through ionization energy losses. In this way, such measurements can be compared with those obtained through simulations, in order to assess the accuracy levels of such simulations and their applicability to quantitative estimates of fragmentation impacts on SEE rates.

III. Trade-off between LET accuracy and absolute magnitude

In addition to the challenges posed by high-energy heavy ion fragmentation, performing accurate and quantitative SEE tests with such beams implies another difficulty, in this case directly related to the way heavy-ions lose energy in matter, reaching their maximum ionization capability (or LET value) at the end of their range. This means that, even if high-energy heavy-ions offer very attractive penetration values in matter, it can be difficult to ensure a high enough LET value at the exact position of the sensitive depth. This can be even more challenging in cases in which multiple sensitive depths are present in a component or assembly (e.g., when testing full boards with multiple chips on them, potentially even on both sides of the board [29]).

This trade-off between the magnitude of the LET value and the accuracy with which it can be determined is depicted in a simplified manner in Fig. 1, in which we have considered a ^{208}Pb beam on silicon of an initial energy of 120 MeV/n, corresponding to a surface LET of 30 MeVcm^2/mg, and where the data of range and LET as a function of ion energy have been extracted from SRIM [30]. As can be seen, an LET of 40 MeVcm^2/mg with a tolerance of $\pm$10% can be ensured over roughly 600 μm, whereas if the LET value is increased to 60 MeVcm^2/mg with the same tolerance requirement, the depth over which the condition is fulfilled is reduced to 230 μm. Whether this is sufficient or not will depend on the accuracy requirements of each test case on the one hand and on the level of accuracy in the knowledge of the overlayer composition and thickness as well as the location of the sensitive area on the other. It has to be noted that the values discussed above consider an ideal scenario, in which energy straggling of the ions (which will increase the LET spread) is not accounted for, and in which only silicon is regarded as a material, whereas more realistically, a significantly more complex structure will apply, likely without a 1D symmetry and with a material budget which can therefore vary depending on the specific ion trajectory.

Note that in Fig. 1, an LET value of 40 (60) MeVcm^2/mg is reached after roughly 1 (2) mm in silicon. However, the depth at which these (or other) values are reached can be tuned through the adjustment of the primary energy, with the

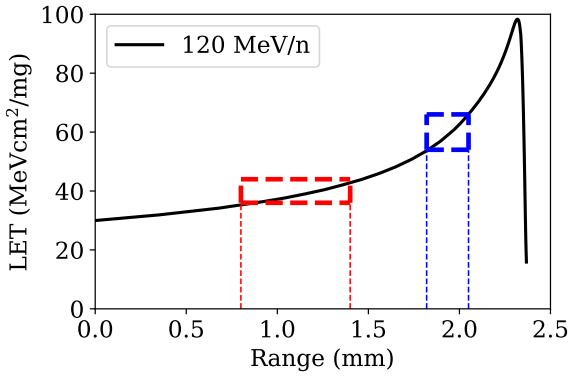

Fig. 1. LET versus range for lead in silicon, with an initial energy of 120 MeV/n, and as retrieved from SRIM [30]. The boxes show a $\pm$10% tolerance around the 40 and 60 MeVcm^2/mg LET values, and include the respective range limits, which become smaller as the LET increases and the ions get closer to the Bragg peak.

main limitations to the approach being (a) the uncertainty in the material composition and thicknesses, as well as in the exact depth value of the sensitive region and (b) the energy straggling and fragmentation the ions will undergo as they interact with matter, which will increase for larger initial energies and ranges.

One way of partially overcoming this trade-off and associated limitation is that of performing subsequent irradiations in which the beam energy, and hence the depth of the Bragg Peak within the tested samples, is varied in small steps [2], [31], [32].

Another way of alleviating the intrinsic trade-off between the LET value that can be reached and the accuracy with which it can be determined is to, as initially proposed in [16], perform tests with fully fragmented high-energy heavy-ion beams. Such beams will be characterized by an LET spectrum as opposed to a single LET value. Moreover, this spectrum will remain fairly constant as it penetrates through electronics components and boards and, as also shown in [16], can be tailored to directly resemble parts of the GCR spectrum.

Therefore, the fragmentation process that was introduced in Section II as a possible source of uncertainty and inaccuracy could be used, if adequately controlled and characterized, to at least partially overcome the trade-off between penetration and LET magnitude applicable to high-energy mono-LET beams. Further discussion about the RHA potential (and limitations) of SEE testing with fully fragmented beams are developed in Section VI of this paper.

IV. Irradiation Facility and Conditions

The experimental results in this study were collected using a 1 GeV/n and 750 MeV/n ^{208}Pb beam from CERN's PS accelerator which, after traveling through several tens of meters of air and a number of beam instruments in the F61 and T8 beam lines, reaches the fragmenter location (consisting of different layers of PMMA of density 1.19 g/cm^3) with a peak energy of 660 MeV/n and 361 MeV/n, respectively. The

fragmenter thickness values for the 660 MeV/n (361 MeV/n) energy were 46, 47, 48, 50, 60 and 78 mm (20 and 40 mm). For both energies, the thinnest fragmenter thickness corresponds to a value just above the range of the beam, meaning that no primary particles are expected to reach the DUT location under these conditions. Interestingly, the maximum fragmenter thickness of 78 mm corresponds to 14.8 g/cm^2, not far from the equivalent thickness of the Martian atmosphere (20 ± 5 g/cm^2) and roughly 1.5% of Earth's atmosphere ($\sim$ 1000 g/cm^2).

A picture of the degrader/fragmenter system and DUT support can be seen in Fig. 2. For reference, the conditions used at GSI through the RADNEXT EU project [33] for the technique introduction and event-by-event energy deposition validation in [16] consisted of an 800 MeV/n uranium beam on 62 mm of PMMA fragmenter (also with a density of 1.19 g/cm^3), and were hence quite similar to the largest of the two energies employed in this work.

Fig. 2. The PMMA degrader and copper masks system, followed by a parallel-plate ionization chamber, and placed roughly 1 m upstream of the Device Under Test location, which is to the right of the plot.

The fragmented ion field generated by the PMMA degraders is simulated using the FLUKA Monte Carlo code [34] by scoring the LET spectrum at the location of the DUT. For the energies and fragmentation reactions relevant to this work, the nucleus-nucleus reactions in FLUKA rely on a modified version of RQMD-2.4 [35] which is a Relativistic Quantum Molecular Dynamic code applied between 125 MeV/n and 5 GeV/n, with results that can be found in [36], [37].

The simulations were performed in two steps. The first consists in transporting particles with an initial energy corresponding to their PS value (i.e., 1 GeV/n in the case we illustrate here) through the transfer and experimental line [38] and scoring the primary beam particles at the level of the degrader system, with an average energy (LET) of 660 MeV/n (13.4 MeVcm^2/mg) and an energy (LET) FWHM spread of 13 MeV/n (0.1 MeVcm^2/mg). All relevant particle properties are recorded and used as input for a second step simulation, focusing fully on the impact of the fragmenter system on the beam properties and yielding as an output the resulting LET spectrum, as shown in detail in Appendix A.

The radiation field at the DUT location has also been measured experimentally by means of its event-by-event energy deposition distribution in a solid-state detector, yielding results in very good agreement with the simulation, and hence serving as a validation. More information about the related radiation field simulations, energy deposition distribution measurements and the comparison between the two are included in [39].

The resulting LET distribution at DUT level for the conditions described above is shown in Fig. 3 in reverse integral form, along with the normalized GCR LET spectrum, to highlight their resemblance in the part of the LET spectrum above the iron knee and extending up to the uranium knee.

This simulated LET distribution will be used in Section V to obtain a calculated SEE rate (or cross section) for the fragmented beams, by folding it with the known SEU cross sections as a function of LET.

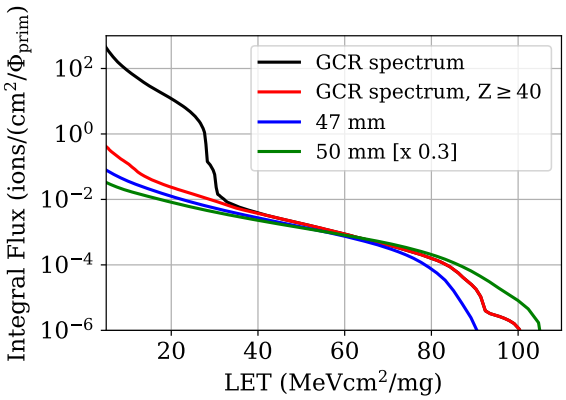

Fig. 3. Reverse integral of the simulated LET spectrum at the DUT location for a 660 MeV/n lead beam on the PMMA fragmenters for thicknesses of 47 and 50 mm. The fragmented spectra are normalized per unit primary fluence (Φ_{prim}), with a factor 0.3 applied to the thinner fragmenter to compensate for the larger secondary ion fluence. The GCR LET spectrum (both full, and limited to ions with Z equal or larger than 40) is also included for reference, normalized arbitrarily to match the absolute value of the spectrum used in this work.

V. SEE Tests and Results

As introduced above, we used a variety of beam, fragmenter and DUT configurations during the 2023 high-energy heavy-ion run at HEARTS@CERN with the purpose of comparing the experimentally obtained SEE rate with that expected from the combination of the fragmented radiation field obtained

through simulations and known LET response of the considered devices and effects. The information about the tested commercial SRAMs is summarized in Table I, along with the Weibull parameters of their heavy ion SEU cross section collected with conventional, mono-LET tests in a variety of facilities, and shown in Fig. 4. As can be seen, while the ISSI and Cypress memories have low LET thresholds (below 1 MeVcm^2/mg) the Renesas memory incorporates critical charge hardening, resulting in an LET threshold of approximately 13 MeVcm^2/mg.

$$\sigma_{frag} = \frac{N_{SEE}}{\Phi_{prim}} = \frac{\int \frac{d\Phi(LET)}{d(LET)} \cdot \sigma(LET) \cdot d(LET)}{\Phi_{prim}} \quad (1)$$

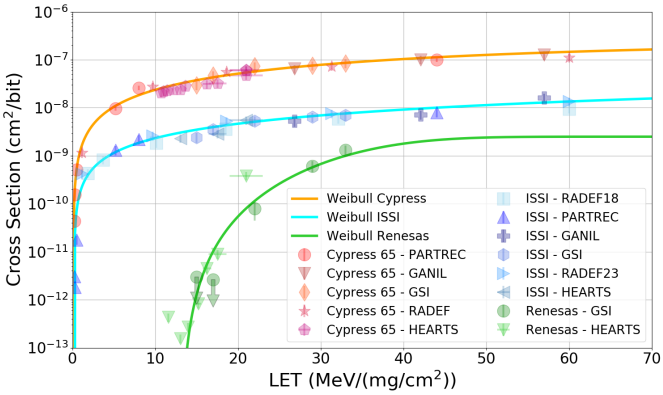

Fig. 4. SEU cross sections as a function of LET for the three memories considered in this work, as collected in multiple heavy-ion facilities.

The SEU tests with the fragmented beam were performed at room temperature, nominal supply voltage (3.3 V) and checkerboard pattern, with the memories being read out every 2.5 s. In each readout cycle, the errors are counted and corrected. As can be seen in the experimental setup in Fig. 5, the Cypress and ISSI memories were tested de-lidded, whereas the Renesas was irradiated with its original packaging. It is to be noted that, as shown in [16] through simulations, the package has a negligible impact on the high-energy ion fragmented field, hence results with and without package are expected to be compatible. The datecodes of the memories were the same as those used to collect the SEU cross section data as a function of LET, therefore the assumption is that all parts of the same reference and datecode have the same (or a very similar) SEU response as a function of LET, which in turn is assumed to fit well to a Weibull function, as supported by Fig. 4. No other SEE effects (e.g., SELs, SEFIs...) were recorded on these memories during the tests with mono-LET or fragmented ion beams.

The SEU results of the SRAMs in the fragmented ion beams are defined as SEU cross sections that take into account the primary fluence [i.e., as per the first part of (1)] even if when reaching the DUT level, the beam is no longer of a mono-energetic, mono-LET nature, but consists rather of a broad spectrum of LET values, as explained in Section IV. However, this is a convenient way of representing the evolution of the SEU cross section (or SEU rate) as a function of depth in a given material for thicknesses larger than the ranges of the primary ion (i.e., beyond its Bragg peak).

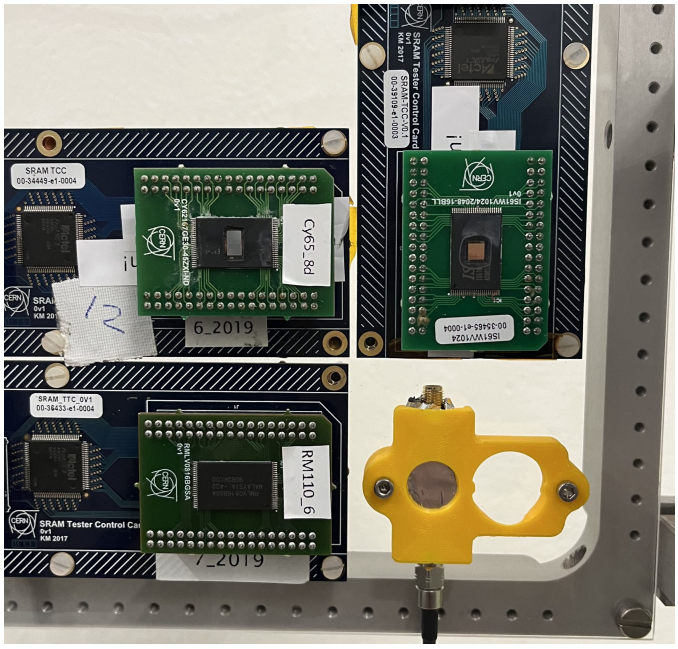

Fig. 5. Experimental setup used to irradiate the three SRAM references with the high-energy heavy-ion fragmented beam. The SRAMs were placed in a remotely movable x-y table and sequentially exposed to the center of the beam. The ISSI (top right) and Cypress (top left) memories were tested de-lidded, whereas the Renesas (bottom left) was tested in its original package. The bottom right position is occupied by a silicon detector, whose results for this same experimental campaign are presented in [39].

The full details of the experimental runs can be found in Appendix B, with the fragmented SEU cross section results for a primary energy of 660 MeV/n plotted in Fig. 6 as a function of the fragmenter thickness.

Before proceeding with the comparison with simulated results, it is worth noting, already solely based on the experimental data, that the SEU cross section (or, equivalently, SEU rate) decreases rapidly after the end-of-range of the heavy ion (corresponding to roughly 45 mm for 660 MeV/n on the PMMA material considered in this work), with a factor of $\sim$ 10 decrease between the SEU cross sections at 40 MeVcm^2/mg and that encountered 5 mm after the end-of-range, i.e., at a depth of 50 mm. Beyond that depth, the reduction follows an exponential law with a rather small attenuation factor, as we will later further analyze and discuss.

In order to compare the experimental fragmented SEU cross section results with those expected from the combination of the simulated LET spectra (see Fig. 3) and SEU cross section as a function of LET (see Fig. 4), we apply the integral in (1) to the simulated spectra for some of the primary energy and fragmenter thickness combinations used experimentally and the three different Weibull response functions from the memories. The related comparison results are shown in Table II, revealing a satisfactory level of agreement, within a factor of 1.5 across the three SRAMs and three fragmenter thicknesses. Moreover, for 78 mm, the ISSI experimental and simulated result are also in perfect agreement and, for the Renesas, the experimental uncertainty related to the low number of counts is

too large to extra from it a meaningful ratio, but the simulated value is also within the (large) experimental interval.

Considering all the possible sources of uncertainty (environment simulation, part-to-part variability, primary beam dosimetry...) this factor of 1.5 agreement over a broad set of conditions is regarded as highly satisfactory.

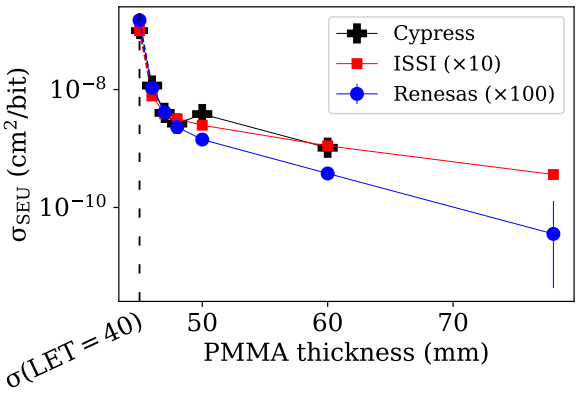

Fig. 6. 660 MeV/n lead beam experimental fragmented SEU cross sections as defined in (1) on different PMMA thicknesses, including the mono-LET value at 40 MeVcm^2/mg for comparison purposes.

VI. Discussion and RHA implications

The two main discussion items of the results described in Section V are illustrated in Fig. 7.

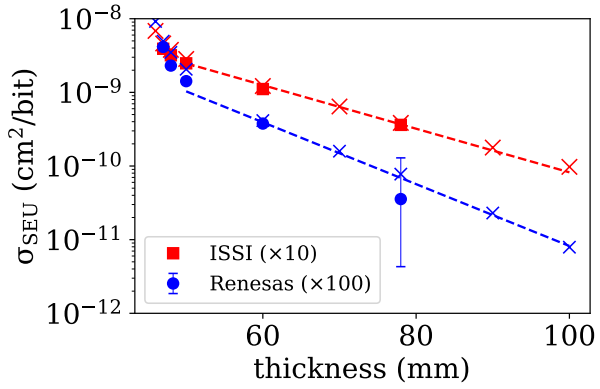

Fig. 7. This figure shows the same experimental data as included in Fig. 6, incorporating also the simulated fragmented SEE cross sections (see Table II) as "X" markers. The dashed lines correspond to the exponential fit to the simulated data as per (2), with the parameters reported in Table III.

The first discussion item is related to the satisfactory level of agreement between simulations and measurements, building confidence for a broader utilization of Monte Carlo calculations to characterize multiple fragmentation conditions combining different primary ion species and energies, as well as material compositions and thicknesses. As previously mentioned and considering the associated uncertainties, this level of agreement in a broad fragmenter thickness range and on memories with very different SEU responses as a function of LET is very positive.

The second discussion item linked to the results is related to the attenuation of the SEE rate as a function of depth which, after the abrupt initial decrease, can be represented analytically by the simple exponential function shown in (2), with the multiplicative factors α and attenuation coefficients m for the three memories shown in Table III (for simplicity, we have used a single fit for the Cypress and ISSI, with a factor of 10 difference in the per-bit cross section, as both of those data sets match very closely, as seen in Fig. 6) and where x refers to the fragmenter thickness.

The inverse of the attenuation coefficient m corresponds to the distance travelled in the material that will reduce the SEU rate by a factor of 10, which corresponds to 33.8 mm in the case of the low-LET threshold memories (Cypress and ISSI) and 23.8 mm for the high-LET threshold device (the Renesas).

$$\sigma_{frag}(x) = \alpha \cdot 10^{-m \cdot x} \tag{2}$$

This relatively inefficient attenuation illustrates the challenge of shielding against SEEs in space, but it can also be seen as an opportunity for ground-level SEE testing with fragmented beams. As introduced in Section III, high-energy mono-LET ion beams will only reach large LET values over relatively limited depths, which can hinder their practical value for SEE testing. However, in the case of fragmented beams and as per (3), it can be seen that, for a condition of $\pm 10\%$ in the SEE rate and assuming the shape of the LET spectrum remains constant, the thickness over which it is achieved is 2.94 mm in the case of the low-LET threshold memories, and 2.08 mm for the high-LET threshold case. Though the comparison is by no means direct, these depths are significantly larger that the 230 µm of $\pm 10\%$ LET value compliance for 60 MeVcm^2/mg illustrated in Fig. 1.

$$x_2 - x_1 = -\frac{\log_{10}\left(\frac{\sigma_{frag}(x_2)}{\sigma_{frag}(x_1)}\right)}{m} \tag{3}$$

Despite its potential, it is worth noting that the possible usage of fragmented heavy ion beams for quantitative SEE testing and qualification would still require substantial development and validation efforts, in relation for instance to the method for quantitatively retrieving an in-orbit rate (or safe operation area) based on ground-level results. In addition, other practical considerations such as the necessary primary fluence (and related beam time) needed to obtain a given fragmented fluence above a certain LET value, as well as the related TID and TNID levels and associated cumulative damage risk, would need to be carefully assessed.

VII. Conclusions and Outlook

In this work we compare experimental and simulated SEU cross section results of three different SRAMs (two with a low LET threshold, and one with a relatively high one) irradiated with a 660 MeV/n lead beam in the HEARTS@CERN facility fragmenting on PMMA (density of 1.19 g/cm^2) thicknesses between 46 and 78 mm. The agreement between simulations

TABLE I
CHARACTERISTICS AND WEIBULL FIT PARAMETERS OF THE SRAM MEMORIES TESTED IN THIS WORK WITH FRAGMENTED HEAVY ION BEAMS. THE RELATED SEU CROSS SECTION DATA ALONG WITH THE WEIBULL FITS CAN BE FOUND IN FIG. 4.

Short Reference	Full Reference	Technology node (nm)	Memory Size (Mbit)	LET_{th} (MeVcm^2/mg)	σ_{sat} (cm^2/bit)	s	W (MeVcm^2/mg)
Cypress	CY62167GE30-45ZXI	65	16	0.1	2.6×10^{-7}	1.2	70
ISSI	IS61WV2048BLL-10TLI	40	32	0.2	1.2×10^{-7}	1	500
Renesas	RMLV0816BGSA-4S2	110	8	13	2.5×10^{-9}	3	25

TABLE II
SEU RATE [I.E., NUMBER OF SEUS PER UNIT PRIMARY ION BEAM FLUENCE AS DEFINED IN (1)] FOR THE THREE SRAMS, AS OBTAINED EXPERIMENTALLY AND THROUGH THE CALCULATION MAKING USE OF THE SIMULATED LET SPECTRA AT THE DUT LOCATION AND THEIR HEAVY-ION CROSS SECTION AS A FUNCTION OF LET. ONLY SBUS ARE USED IN THE DERIVATION OF BOTH THE EXPERIMENTAL AND CALCULATED SEU RATES. THE RATIO BETWEEN THE CALCULATED AND EXPERIMENTAL SEU CROSS SECTIONS ARE ALSO INCLUDED, EXCEPT FOR THE RENESAS MEMORY AND 78 MM, FOR WHICH THE UNCERTAINTY OF THE EXPERIMENTAL VALUE IS TOO LARGE TO EXTRACT A MEANINGFUL RATIO, BUT FOR WHICH THE SIMULATION VALUE LIES WITHIN THE EXPERIMENTAL INTERVAL.

Reference	Fragmenter Thickness (mm)	Calculated (cm^2/bit)	Experimental (cm^2/bit)	Ratio
Cypress	47	4.81×10^{-9}	4.02×10^{-9}	1.20
ISSI		4.61×10^{-10}	3.91×10^{-10}	1.17
Renesas		4.96×10^{-11}	4.14×10^{-11}	1.20
Cypress	50	2.90×10^{-9}	3.84×10^{-9}	0.76
ISSI		2.84×10^{-10}	2.48×10^{-10}	1.15
Renesas		2.06×10^{-11}	1.42×10^{-11}	1.45
Cypress	60	1.19×10^{-9}	1.03×10^{-9}	1.16
ISSI		1.22×10^{-10}	1.11×10^{-10}	1.10
Renesas		4.14×10^{-12}	3.77×10^{-12}	1.17
ISSI	78	3.85×10^{-11}	3.62×10^{-11}	1.06
Renesas		7.76×10^{-13}	$[0.43 - 12.9] \times 10^{-13}$	-

TABLE III
FACTORS FOR THE EXPONENTIAL FITS OF THE FRAGMENTED SEU CROSS SECTION ATTENUATION AS A FUNCTION OF DEPTH, AS DEFINED IN (2) AND SHOWN IN FIG. 7.

Reference	α (cm^2/bit)	m (mm^{-1})
Cypress	7.49×10^{-8}	0.0296
ISSI	7.49×10^{-9}	0.0296
Renesas	1.30×10^{-9}	0.0420

and experiments is satisfactory (i.e., within a factor of 1.5) over all three memories and fragmenter thicknesses and shows that, after a relatively fast attenuation of the SEU cross section (or rate) beyond the ranging out of the primary ions (factor of $\sim$10 attenuation over $\sim$5 mm), the attenuation for thicker values very well follows an exponential decay with a relatively small attenuation factor, meaning that further factors of 10 reductions require 34 mm in the case of the low-LET thershold memories, and 24 mm for the high-LET threshold memory.

Such results illustrate the challenges of shielding against energetic ions, even for thicknesses beyond their range, but also motivate the possible use of high-energy heavy ion beams for high-penetration, high-LET ground-level testing. However, such possibility would require further development and validation efforts before reaching the maturity level required for quantitative electronics testing, and could be the subject of future work.

Other possibilities of expanding the results and discussions presented in this paper are to more broadly characterize the high-energy ion fragmentation and its impact on SEEs, both experimentally and through simulations, for a larger set of primary energies, ion species, fragmenter materials and thicknesses, and SEE and device types.

APPENDIX A
FRAGMENTED HIGH-ENERGY HEAVY ION SIMULATIONS

Once confirmed that the spread in the primary beam energy as obtained in the first step simulation does not play a relevant role in the fragmentation (FWMH/E_0 < 2%), the second step of the simulation is performed with a monoenergetic lead beam at 660 MeV/n. In this case, the geometry is a simple layer of PMMA material of variable thickness (46-78 mm), followed by a layer of air compatible to the actual distance in the tests (180 cm approx.) The beam structure is Gaussian with FWMH 10 cm, as both predicted in the simulations and measured experimentally, and the fluence is scored as a function of the LET in concentric circles to obtain the dependence with the radial distance in the DUT position. The fluence scoring considered in the plots below and related SEE rate calculations corresponds to that at the center of the beam downstream the fragmenter, with a scoring radius of 1 mm. Given the relatively large size of the beam, the flux can be considered as homogeneous over the tested DUT surfaces.

The resulting LET distributions obtained at DUT level are shown in Fig. 8, in reverse integral format. As can be seen, the increasing PMMA material thickness has the coupled effect of (a) reducing the ion fluences and (b) shifting the distributions to lower LET values.

All values are normalized per unit primary fluence meaning that, for instance, in order to obtain an integral fluence of 10^6 ions/cm^2 above 20 MeVcm^2/mg for the 50 mm fragmenter

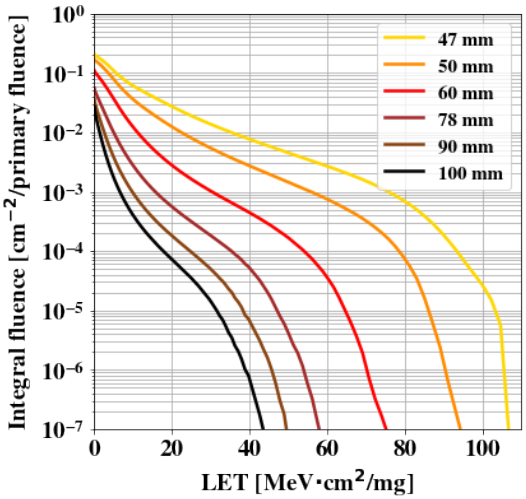

Fig. 8. Reverse integral of the simulated LET spectrum after different fragmenter thicknesses, normalized to the primary fluence.

thickness, a primary fluence of approximately 10^8 ions/cm^2 is needed.

Moreover, the effect of the distribution shift towards lower LETs is shown in Fig. 9, where all curves are normalized to their fluence above 40 MeVcm^2/mg, at which point and by construction all distributions have equal normalized values.

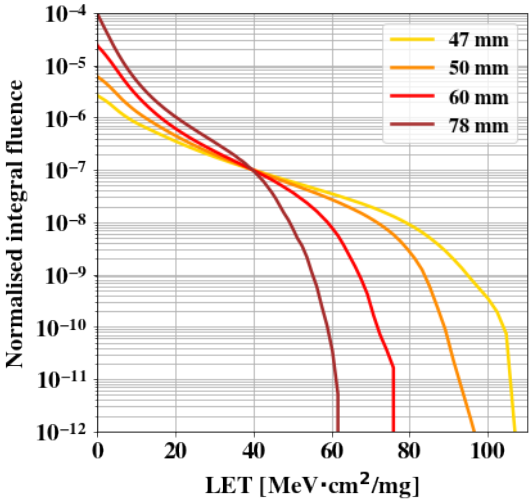

Fig. 9. Same plot as Fig. 8 but normalized in addition by the fluence above 40 MeVcm^2/mg to better observe the evolution of the LET distribution as a function of depth, independently of the fluence reduction. Only thicknesses up to 78 mm are considered due to the small fraction of heavy ions above 40 MeVcm^2/mg for larger thicknesses.

These LET distributions can be integrated with the Weibull response functions shown in Fig. 4 in order to obtain the simulated fragmented SEU cross sections, as per (1), and resulting in the values shown in Table IV.

TABLE IV
SIMULATED SEU CROSS SECTIONS FOR FRAGMENTED BEAMS, OBTAINED BY COMBINING THE WEIBULL FITS IN FIG. 4 AND THE SIMULATED SPECTRA SHOWN IN FIG. 8 BY MEANS OF (1).

Reference	Fragmenter Thickness (mm)	Calculated (cm^2/bit)
Cypress	46	7.16×10^{-9}
ISSI		6.83×10^{-10}
Renesas		9.19×10^{-11}
Cypress	47	4.81×10^{-9}
ISSI		4.61×10^{-10}
Renesas		4.96×10^{-11}
Cypress	48	3.92×10^{-9}
ISSI		3.78×10^{-10}
Renesas		3.49×10^{-11}
Cypress	50	2.90×10^{-9}
ISSI		2.84×10^{-10}
Renesas		2.06×10^{-11}
Cypress	60	1.19×10^{-9}
ISSI		1.22×10^{-10}
Renesas		4.14×10^{-12}
Cypress	70	6.14×10^{-10}
ISSI		6.43×10^{-11}
Renesas		1.59×10^{-12}
Cypress	78	3.61×10^{-10}
ISSI		3.85×10^{-11}
Renesas		7.76×10^{-13}
Cypress	90	1.61×10^{-10}
ISSI		1.78×10^{-11}
Renesas		2.30×10^{-13}
Cypress	100	8.61×10^{-11}
ISSI		9.74×10^{-12}
Renesas		7.90×10^{-14}

APPENDIX B
FRAGMENTED HIGH-ENERGY HEAVY ION RUNS DURING THE 2023 HEARTS@CERN CAMPAIGN

The experimental data used in this work and summarized in Table V were collected between October 21 and 27, 2023, during the 2-week HEARTS@CERN campaign. SEU cross sections are based on the number of Single Bit Upset (SBU) counts, however Multiple Bit Upsets (MBUs) are included in the table for completeness. With the exception of Run 143 for the ISSI, all ISSI and Cypress runs have a very low number of MBUs in relation to the SBUs, which could even be of statistical origin, owing to the large number of total counts involved. However, for the Renesas memory, which uses a hardening technique similar to the one analyzed in [40], the amount of MBUs relative to the SBUs is significant, and could be a subject of future study. It is worth noting that a large fraction of MBUs was recorded with this component also in the mono-LET tests.

ACKNOWLEDGEMENTS

The authors acknowledge the CHARM and IRRAD teams as well as the PS Operations, Radiation Protection, Beam Instrumentation and Sources, Targets and Interaction groups for their critical support related to the high-energy heavy-ion experimental runs at CERN.

REFERENCES

[1] HEARTS EU-project website, accessed 30-Jan-2024. [Online]. Available: https://hearts-project.eu/

TABLE V
MEASURED PRIMARY ION FLUENCES, SINGLE BIT UPSETS AND MULTIPLE BIT UPSETS FOR THE THREE CONSIDERED SRAM MEMORIES DURING THEIR FRAGMENTED BEAM RUNS. IN THE CASE OF RUN 62 AND GIVEN THE VERY LOW COUNTS STATISTICS, THE 95% CONFIDENCE LEVEL INTERVAL OF THE MEASUREMENT IS GIVEN.

Reference	Beam Energy (MeV/n)	Run ID	Degrader thickness (mm)	Fluence (cm^{-2})	Run Duration (s)	SBU	MBU	σ_{frag} (cm^2/bit)
Cypress	361	77	20	2.04×10^4	641	946	0	$(2.71 \pm 0.54) \times 10^{-9}$
	660	96	46	5.21×10^3	359	1020	0	$(1.17 \pm 2.33) \times 10^{-8}$
		97	47	4.15×10^3	345	280	0	$(4.02 \pm 0.86) \times 10^{-9}$
		98	48	2.74×10^3	293	121	0	$(2.64 \pm 0.53) \times 10^{-9}$
		99	50	3.36×10^3	321	216	0	$(3.84 \pm 0.77) \times 10^{-9}$
		100	60	5.74×10^3	645	99	0	$(1.03 \pm 0.21) \times 10^{-9}$
ISSI	361	124	20	5.66×10^5	289	3144	0	$(1.66 \pm 0.33) \times 10^{-10}$
		125	40	1.16×10^6	612	215	0	$(5.52 \pm 1.11) \times 10^{-12}$
	660	143	46	1.22×10^6	257	32263	1002	$(7.85 \pm 1.57) \times 10^{-10}$
		144	47	1.28×10^6	261	16839	3	$(3.91 \pm 0.78) \times 10^{-10}$
		145	48	1.30×10^6	255	13948	5	$(3.19 \pm 0.64) \times 10^{-10}$
		146	50	1.42×10^6	292	11789	0	$(2.48 \pm 0.50) \times 10^{-10}$
		147	60	1.57×10^6	313	5826	0	$(1.11 \pm 0.22) \times 10^{-10}$
		148	78	3.01×10^6	606	3657	0	$(3.62 \pm 0.72) \times 10^{-11}$
Renesas	361	69	20	9.76×10^5	513	184	47	$(2.25 \pm 0.45) \times 10^{-11}$
	660	57	46	8.81×10^5	210	790	290	$(1.07 \pm 0.21) \times 10^{-10}$
		58	47	7.92×10^5	195	275	45	$(4.14 \pm 0.83) \times 10^{-11}$
		59	48	1.21×10^6	286	234	32	$(2.31 \pm 0.46) \times 10^{-11}$
		60	50	1.24×10^6	286	147	20	$(1.42 \pm 0.29) \times 10^{-11}$
		61	60	2.69×10^6	632	85	7	$(3.77 \pm 0.76) \times 10^{-12}$
		62	78	6.69×10^5	157	2	0	$[0.43 - 12.9] \times 10^{-13}$

[2] S. Buchner, N. Kanyogoro, D. McMorrow, C. C. Foster, P. M. O'Neill, and K. V. Nguyen, "Variable depth Bragg peak method for single event effects testing," *IEEE Trans. Nucl. Sci.*, vol. 58, no. 6, pp. 2976–2982, Dec 2011.

[3] C. La Tessa, M. Sivertz, I.-H. Chiang, D. Lowenstein, and A. Rusek, "Overview of the NASA space radiation laboratory," *Life Sci. Space Res.*, vol. 11, pp. 18–23, Nov. 2016.

[4] M. A. Fraser *et al.*, "Feasibility of slow-extracted high-energy ions from the CERN Proton Synchrotron for CHARM," presented at IPAC'22, Bangkok, Thailand, Jun. 2022.

[5] E. Johnson, M. Fraser, M. Delrieux, R. G. Alia, K. Bilko, A. Waets *et al.*, "Beam delivery of high-energy ion beams for irradiation experiments at the CERN proton synchrotron," in *Proc. 14th Int. Part. Accel. Conf. Geneva, Switzerland: JACoW Publishing*, May 2023, pp. 297–300.

[6] E. Johnson, A. Bilko, M. Delrieux, L. Esposito, N. Emriskova, and M. Fraser, "Beam optics modelling of slow-extracted very high-energy heavy ions from the CERN Proton Synchrotron for radiation effects testing," *Proc. IPAC'24, (Nashiville TN, USA)*, pp. 3554–3557, 2024.

[7] K. Bilko, R. G. Alía, A. Costantino, A. Coronetti, S. Danzeca, M. Delrieux *et al.*, "CHARM high-energy ions for microelectronics reliability assurance (CHIMERA)," *IEEE Trans. Nucl. Sci.*, vol. 71, no. 8, pp. 1549–1556, Aug 2024.

[8] P. Fernández-Martínez, R. G. Alía, M. Cecchetto, M. Kastriotou, N. Kerboub, M. Tali *et al.*, "SEE tests with ultra energetic Xe ion beam in the CHARM facility at CERN," *IEEE Trans. Nucl. Sci.*, vol. 66, no. 7, pp. 1523–1531, Mar. 2019.

[9] R. G. Alía, P. F. Martínez, M. Kastriotou, M. Brugger, J. Bernhard, M. Cecchetto *et al.*, "Ultraenergetic heavy-ion beams in the CERN accelerator complex for radiation effects testing," *IEEE Trans. Nucl. Sci.*, vol. 66, no. 1, pp. 458–465, Jan 2019.

[10] N. Emriskova, A. Waets, O. De La Ruë Du, K. Klimek, and R. García Alía, "Characterisation of degraded very-high-energy heavy ion beams using the HEARTS LET booster," *IEEE Trans. Nucl. Sci.*, vol. Early Access, 2025, doi: 10.1109/TNS.2024.3521185.

[11] A. Waets, N. Emriskova, V. Pan, A. Rosenfeld, L. Tran, J. Vohradsky *et al.*, "Microdosimetry of very-high-energy heavy ion beams for electronics testing using silicon-on-insulator detectors," *IEEE Trans. Nucl. Sci.*, submitted for publication.

[12] A. Pflaum, M. Lapp, B. Poppe, A. Waets, N. Emriskova, E. Johnson *et al.*, "Characterisation of a ^{208}Pb heavy ion beam at CHARM," *IEEE Trans. Nucl. Sci.*, submitted for publication.

[13] A. Coronetti, R. García-Alía, L. Dilillo, C. Imianosky, D. A. Dos Santos, L. M. Luza *et al.*, "SRAM-based heavy ion beam flux and LET dosimetry," *IEEE Trans. Nucl. Sci.*, vol. Early Access, 2024, doi: 10.1109/TNS.2024.3487647.

[14] A. Coronetti, M. S. Barbero, K. Bilko, N. Emriskova, E. Johnson, K. M. Klimek *et al.*, "Results of single event effect testing at the new HEARTS@CERN high-energy heavy ion facility at CERN," in *2024 IEEE Radiation Effects Data Workshop (REDW) (in conjunction with 2024 NSREC)*, 2024.

[15] J. R. Schwank, M. R. Shaneyfelt, and P. E. Dodd, "Radiation hardness assurance testing of microelectronic devices and integrated circuits: Test guideline for proton and heavy ion single-event effects," *IEEE Trans. Nucl. Sci.*, vol. 60, no. 3, pp. 2101–2118, Jun 2013.

[16] R. G. Alía, K. Bilko, F. Cerutti, A. Coronetti, N. Emriskova, L. Esposito *et al.*, "Fragmented high-energy heavy-ion beams for electronics testing," *IEEE Trans. Nucl. Sci.*, vol. 70, no. 4, pp. 486–495, Apr 2023.

[17] M. A. Clemens, N. A. Dodds, R. A. Weller, M. H. Mendenhall, R. A. Reed, R. D. Schrimpf *et al.*, "The effects of nuclear fragmentation models on single event effect prediction," *IEEE Trans. Nucl. Sci.*, vol. 56, no. 6, pp. 3158–3164, Dec 2009.

[18] K. Warren, R. Weller, M. Mendenhall, R. Reed, D. Ball, C. Howe *et al.*, "The contribution of nuclear reactions to heavy ion single event upset cross-section measurements in a high-density SEU hardened SRAM," *IEEE Trans. Nucl. Sci.*, vol. 52, no. 6, pp. 2125–2131, Dec 2005.

[19] C. Howe, R. Weller, R. Reed, M. Mendenhall, R. Schrimpf, K. Warren *et al.*, "Role of heavy-ion nuclear reactions in determining on-orbit single event error rates," *IEEE Trans. Nucl. Sci.*, vol. 52, no. 6, pp. 2182–2188, Dec 2005.

[20] R. A. Reed, R. A. Weller, M. H. Mendenhall, J.-M. Lauenstein, K. M. Warren, J. A. Pellish *et al.*, "Impact of ion energy and species on single event effects analysis," *IEEE Trans. Nucl. Sci.*, vol. 54, no. 6, pp. 2312–2321, Dec 2007.

[21] P. E. Dodd, J. R. Schwank, M. R. Shaneyfelt, J. A. Felix, P. Paillet, V. Ferlet-Cavrois *et al.*, "Impact of heavy ion energy and nuclear interactions on single-event upset and latchup in integrated circuits," *IEEE Trans. Nucl. Sci.*, vol. 54, no. 6, pp. 2303–2311, Dec 2007.

[22] V. Ferlet-Cavrois, J. R. Schwank, S. Liu, M. Muschitiello, T. Beutier, A. Javanainen *et al.*, "Influence of beam conditions and energy for SEE testing," *IEEE Trans. Nucl. Sci.*, vol. 59, no. 4, pp. 1149–1160, Aug 2012.

[23] R. García Alía, C. Bahamonde, S. Brandenburg, M. Brugger, E. Daly, V. Ferlet-Cavrois *et al.*, "Sub-LET threshold SEE cross section dependency with ion energy," *IEEE Trans. Nucl. Sci.*, vol. 62, no. 6, pp. 2797–2806, Dec 2015.

[24] R. García Alía, M. Brugger, V. Ferlet-Cavrois, S. Brandenburg, J.

Calcutt, F. Cerutti *et al.*, "Proton dominance of sub-LET threshold GCR SEE rate," *IEEE Trans. Nucl. Sci.*, vol. 64, no. 1, pp. 388–397, Jan 2017.

[25] M. Kastriotou, P. Fernandez-Martinez, R. G. Alía, C. Cazzaniga, M. Cecchetto, A. Coronetti *et al.*, "Single event effect testing with ultrahigh energy heavy ion beams," *IEEE Trans. Nucl. Sci.*, vol. 67, no. 1, pp. 63–70, Jan 2020.

[26] M. Sacristán Barbero, I. Slipukhin, M. Cecchetto, D. Prelipcean, Y. Aguiar, K. Bilko *et al.*, "Characterization of fragmented ultrahigh-energy heavy ion beam and its effects on electronics single-event effect testing," *IEEE Trans. Nucl. Sci.*, vol. 71, no. 8, pp. 1557–1564, Aug 2024.

[27] V. Wyrwoll, R. G. Alia, K. Røed, C. Cazzaniga, M. Kastriotou, P. Fernández-Martínez *et al.*, "Longitudinal direct ionization impact of heavy ions on SEE testing for ultrahigh energies," *IEEE Trans. Nucl. Sci.*, vol. 67, no. 7, pp. 1530–1539, Jul 2020.

[28] V. Wyrwoll, B. Delfs, M. Lapp, D. Poppinga, P. Fernandéz Martinéz, M. Kastriotou *et al.*, "On-line beam monitoring and dose profile measurements of a ^{208}Pb beam of 150 GeV/n with a liquid-filled ionization chamber array," *Nucl. Instrum. Methods Phys. Res., Sect. A*, vol. 987, no. 164831, Jan 2021.

[29] A. de Bibikoff and P. Lamberbourg, "Method for system-level testing of COTS electronic board under high-energy heavy ions," *IEEE Trans. Nucl. Sci.*, vol. 67, no. 10, pp. 2179–2187, Oct 2020.

[30] J. F. Ziegler, M. Ziegler, and J. Biersack, "SRIM – the stopping and range of ions in matter (2010)," *Nucl. Instrum. Methods Phys. Res., Sect. B*, vol. 268, no. 11, pp. 1818–1823, Jun 2010, 19th International Conference on Ion Beam Analysis.

[31] C. C. Foster, P. M. O'Neill, B. D. Reddell, K. V. Nguyen, B. H. Jones, N. J.-M. Roche *et al.*, "Certification of parts for space with the variable depth Bragg peak method," *IEEE Trans. Nucl. Sci.*, vol. 59, no. 6, pp. 2909–2913, Dec 2012.

[32] N. J.-H. Roche, S. P. Buchner, C. C. Foster, M. P. King, N. A. Dodds, J. H. Warner *et al.*, "Validation of the variable depth Bragg peak method for single-event latchup testing using ion beam characterization," *IEEE Trans. Nucl. Sci.*, vol. 61, no. 6, pp. 3061–3067, Dec 2014.

[33] R. G. Alía, A. Coronetti, K. Bilko, M. Cecchetto, G. Datzmann, S. Fiore *et al.*, "Heavy ion energy deposition and SEE intercomparison within the RADNEXT irradiation facility network," *IEEE Trans. Nucl. Sci.*, vol. 70, no. 8, pp. 1596–1605, Aug 2023.

[34] C. Ahdida, D. Bozzato, D. Calzolari, F. Cerutti, N. Charitonidis, A. Cimmino *et al.*, "New capabilities of the FLUKA multi-purpose code," *Front. Phys*, vol. 9, no. 788253, Jan 2022.

[35] H. Sorge, H. Stöcker, and W. Greiner, "Poincaré invariant Hamiltonian dynamics: Modelling multi-hadronic interactions in a phase space approach," *Ann. Phys.*, vol. 192, no. 2, pp. 266–306, Jun 1989.

[36] V. Andersen, F. Ballarini, G. Battistoni, M. Campanella, M. Carboni, F. Cerutti *et al.*, "The FLUKA code for space applications: recent developments," *Adv. Space Res.*, vol. 34, no. 6, pp. 1302–1310, Jan 2004.

[37] H. Aiginger, V. Andersen, F. Ballarini, G. Battistoni, M. Campanella, M. Carboni *et al.*, "The FLUKA code: new developments and application to 1 GeV/n iron beams," *Adv. Space Res.*, vol. 35, no. 2, pp. 214–222, Jan 2005.

[38] A. Waets, K. Bilko, D. Brethoux, F. Cerutti, N. Charitonidis, M. Delrieux *et al.*, "Heavy ion beam characterization for radiation effects testing at CERN using Monte Carlo simulations and experimental benchmarking," in *Proc. 14th Int. Part. Accel. Conf. Geneva, Switzerland: JACoW Publishing*, May 2023, pp. 5165–5168.

[39] A. Waets, R. G. Alia, K. Bilko, N. Emriskova, L. S. Esposito, C. Schuy *et al.*, "Characterization of fully fragmented high-energy heavy ion beams for see testing through measurements and simulations," *IEEE Trans. Nucl. Sci.*, vol. Early Access, Nov 2024, doi: 10.1109/TNS.2024.3492039.

[40] S. Uznanski, R. G. Alia, E. Blackmore, M. Brugger, R. Gaillard, J. Mekki *et al.*, "The effect of proton energy on SEU cross section of a 16 mbit TFT PMOS SRAM with DRAM capacitors," *IEEE Trans. Nucl. Sci.*, vol. 61, no. 6, pp. 3074–3079, Dec 2014.